

# Experimental Investigation of Spacecraft In-Flight Disturbances and Dynamic Response

Stanley E. Woodard\*

*NASA Langley Research Center, Hampton, Virginia 23681-0001*

Richard R. Lay<sup>†</sup> and Robert F. Jarnot<sup>†</sup>

*Jet Propulsion Laboratory, California Institute of Technology, Pasadena, California 91109-8099*  
and

David A. Gell<sup>‡</sup>

*University of Michigan, Ann Arbor, Michigan 48109-2143*

In September 1991, NASA launched the Upper Atmosphere Research Satellite. In addition to its atmospheric sciences mission, analysis of data from the first 370 days after launch was used to investigate in-flight spacecraft disturbances and responses. The investigation included a three-orbit in-flight experiment to determine how each onboard instrument and subsystem disturbance contributed to the overall spacecraft dynamic response. The investigation quantified the spacecraft dynamic response produced by the solar array and high-gain antenna harmonic drive disturbances. The solar array's harmonic drive output resonated two solar array modes. Friction in the solar array gear drive provided sufficient energy dissipation, which prevented the solar panels from resonating catastrophically; however, the solar array vibration amplitude was excessively large. The resulting vibration had a latitude-specific pattern. Thermal elastic bending of the spacecraft's two flexible appendages as the spacecraft crosses the Earth's terminator and solar array modal contribution to the spacecraft response were also examined.

## Nomenclature

$N_{HD}$	= harmonic drive speed reduction ratio
$N_{SG}$	= spur gear speed reduction ratio
$\beta$	= complement of the angle between the orbit normal and the Earth-to-sun vector, deg
$\dot{\theta}$	= payload rotational speed, deg/s
$\omega_{HD}$	= harmonic drive output frequency, Hz

## Introduction

ON Sept. 12, 1991, NASA launched the Upper Atmosphere Research Satellite (UARS). The goal of UARS was to carry out the first systematic, comprehensive study of the stratosphere and to furnish new data on the mesosphere and thermosphere. UARS provided critical data on the chemical composition of the upper atmosphere, particularly the structure of the Earth's protective ozone layer in the stratosphere. This satellite mission was the first element of a long-term national program to study global atmospheric change.

In addition to its atmospheric sciences mission, data from the first 370 days past the launch of UARS were used to investigate in-flight spacecraft dynamics. Figures 1 and 2 show the spacecraft in prelaunch and operating configurations, respectively. Although the UARS spacecraft was used in this study, identification and measurement of spacecraft disturbances and their respective response can be used to increase the accuracy of prelaunch predictions on many spacecraft.<sup>1-7</sup> Furthermore, as instrument pointing requirements become more demanding, spacecraft disturbances that were

previously unimportant are becoming limiting factors in the quality of science data. The investigation also included a three-orbit in-flight experiment using UARS.

Objectives of the experiment were to isolate all disturbances known before launch, create disturbance combinations, create spacecraft dynamic responses suitable for system identification, examine spacecraft quiescence, and identify any disturbances not known before launch. A primary goal of the experiment was to determine how each instrument and subsystem disturbance contributed to the overall spacecraft dynamic response. The experiment was conducted during the last four hours of May 1, 1992 [233rd day after launch, Greenwich mean time (GMT)], 5 h after the spacecraft had rotated 180 deg about its yaw axis. Analysis of flight data before the experiment indicated that the solar array edgewise and flatwise modes were constantly excited. Prelaunch analysis indicated that the Microwave Limb Sounder (Fig. 1) antenna limb viewing scan profile was the excitation source. Thus, the experiment provided a means to identify the solar array excitation source.

This paper presents analysis results from the experiment and flight data from the 133rd, 139th, 265th, 266th, and 370th days after launch. Following an overview of the spacecraft, results are presented that show solar array drive, solar array modal, high-gain antenna drive, and appendage thermal-elastic bending contribution to the spacecraft dynamic response.

## UARS Overview

The UARS satellite (Figs. 1 and 2) consisted of 10 science instruments mounted on an instrument module attached to a modular spacecraft. The modular spacecraft provided attitude control, communication and data handling, electrical power distribution, and propulsion. A high-gain antenna mounted on the instrument module was used for communication to the two tracking data and relay satellites. Also mounted on the instrument module was a suite of three instruments, which shared the same gimbal mount (Solar/Stellar Pointing Platform) and a solar array with six panels. The satellite had two elastically flexible appendages (solar array and instrument boom) that could be excited by multiple disturbance sources onboard the spacecraft. The onboard disturbances were caused by five gimballed instruments and subsystems, the solar array, the reaction wheels, the propulsion subsystem, and thermal elastic bending

Received Nov. 21, 1995; revision received Jan. 2, 1997; accepted for publication Jan. 3, 1997. Copyright © 1997 by the American Institute of Aeronautics and Astronautics, Inc. No copyright is asserted in the United States under Title 17, U.S. Code. The U.S. Government has a royalty-free license to exercise all rights under the copyright claimed herein for Governmental purposes. All other rights are reserved by the copyright owner.

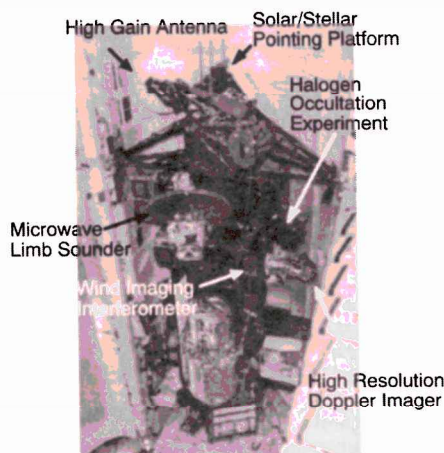
\*Senior Research Engineer, Structural Dynamics Branch, Structures Division, MS 230, Member AIAA.

<sup>†</sup>Member, Technical Staff, Microwave, Lidar, and Interferometer Technology Section, Observational Systems Division, 4800 Oak Grove Drive, Mail-Stop 183-701.

<sup>‡</sup>Senior Research Associate, Space Physics Research Laboratory, Department of Atmospheric, Oceanic and Space Sciences, 2455 Hayward Street.

**Table 1** UARS disturbances known before launch

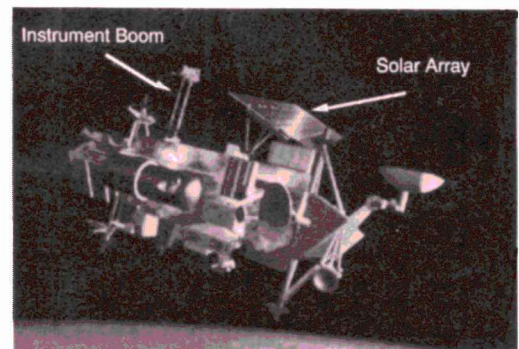
Disturbance	Description	Trigger
Thermal snap	Thermal elastic bending of solar array due to rapidly changing thermal environment	Terminator crossing
Halogen Occultation Experiment (HALOE) sunrise and sunset occultation measurements	HALOE unstows, targets and tracks sun through atmosphere then stows	Orbital sunrise and sunset
Microwave Limb Sounder (MLS) antenna	Approx. 27 forward steps followed by 2 rewind steps	Continuously repeated throughout orbit
MLS switching mirror	Rapid slew/stop through 3 positions	Continuously repeated throughout orbit
Solar/Stellar Pointing Platform	Positions, stops, targets (sun or stellar target), stops, positions for next target	Position of sun or stellar target
High Gain Antenna	Positions, stops, targets Tracking and Data Relay Satellite (TDRS), stops, positions for next TDRS	TDRS (east or west) positions
Solar array stopping and rewinding	Changing direction of solar array rotation	Yaw maneuver completion
High Resolution Doppler Imager (HRDI) day/night scan transition	Rapid rotation of azim. and elev. gimbals.	Orbital sunrise and sunset
HRDI day/night scans	Elev. rotation (down) followed by 90-deg azim. rotation followed by elev. rotation (up)	Continuous repeated day scans from sunrise to sunset. Same for night scans (sunset to sunrise)
Reaction wheels	Performs attitude changes, stability and momentum management	Change in attitude and rate; commanded attitude biases
Magnetic torques	Provides reaction wheel momentum unloading	Excessive change in attitude rate
Propulsion subsystem	Thrust to spacecraft using hydrazine propulsion module	Orbit adjustments. Also used in conjunction with magnetic torques to unload reaction wheels

**Fig. 1** UARS in the bay of the Space Shuttle Discovery (STS-48).

(thermal snap) of the flexible appendages as the spacecraft passed through the Earth's terminator.

The UARS attitude control system had a number of onboard sensors for attitude determination; however, only the rate gyros in the Inertial Reference Unit could determine attitude to the precision needed in this study. These gyros had a resolution of 0.05 arc-s (one gyro count) and a sampling rate of 7.8125 Hz. Attitude time histories were developed by integrating the gyro data. The attitude times histories were used to develop jitter time histories. Jitter is the angular excursion of an instrument's line of sight in a reference time interval (such as a sampling time period).<sup>1</sup>

Table 1 describes disturbances known before launch that were expected to have had a measurable impact on spacecraft jitter.<sup>8-12</sup> Many of these disturbances were triggered by the spacecraft's position in orbit such as thermal snap of the solar array or Halogen Occultation Experiment measurement events during orbital sunrise and sunset.<sup>2,11,12</sup> Some disturbances were the result of the position of UARS relative to other spacecraft such as the line of sight of the

**Fig. 2** Artist concept of UARS on orbit.

high-gain antenna to the Tracking and Data Relay Satellites (east and west) in geostationary orbits.<sup>2,3</sup> Other disturbances, which were assumed to be negligible, were caused by the drive mechanisms of the science instruments and subsystems. Reference 7 provides more detailed discussion of UARS and its in-flight dynamics during a typical orbit.

Figure 3 shows instrument, subsystem, and structural frequencies below 4.0 Hz. Structural frequencies are numbered (Refs. 5 and 7 have descriptions of the frequencies) and system/instrument frequencies are annotated. The attitude control system had a bandwidth of 0.011 Hz with a rolloff of 36 dB/decade.<sup>2,13</sup> The attitude control system partially attenuated disturbances caused by the rewind of the Microwave Limb Sounder antenna. A band from approximately 0.2–0.3 Hz represents the solar array modal frequency variations for the solar array edgewise and flatwise modes. The variations were caused by the solar array rotating through a complete revolution.<sup>4,5,7</sup> Harmonic drive output frequencies for the Solar/Stellar Pointing Platform, the solar array, and the high-gain antenna during their targeting maneuvers are also within the frequency band of the solar array modes. Thus, during separate parts of an orbit, the subsystems resonated both the solar array flatwise and edgewise modes.

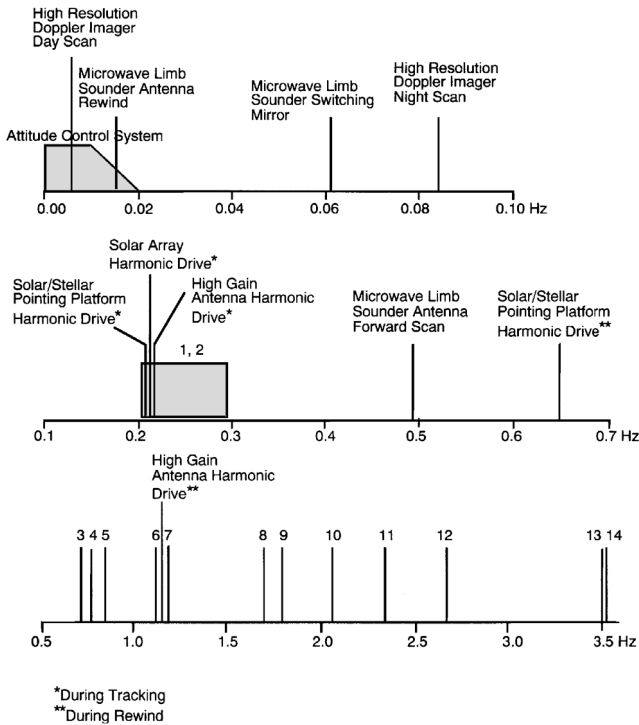


Fig. 3 UARS structural and instrument frequencies below 4.0 Hz.

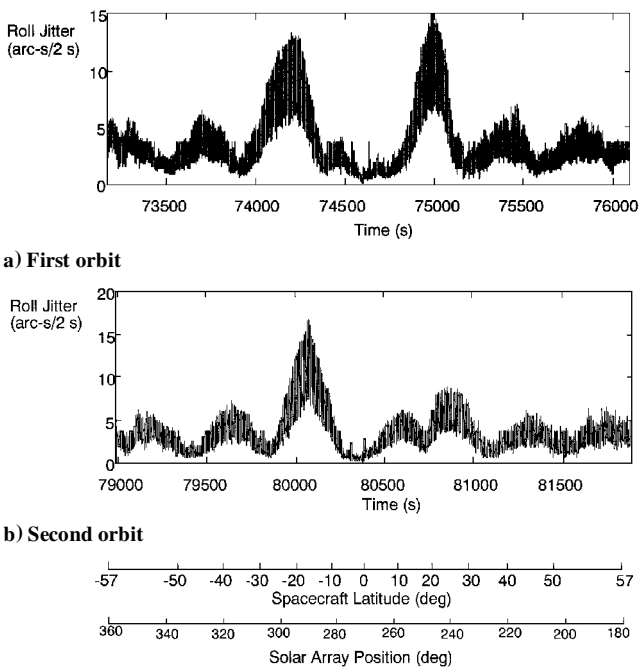


Fig. 4 Roll jitter at latitudes 57°S to 57°N during ascending part of both orbits in the experiment.

### Solar Array Drive Contribution to Spacecraft Dynamic Response

One of the first results from the May 1 experiment was the unexpected vibration level of the edgewise and flatwise modes and the 5-min beats dominating roll and yaw responses. The Wind Imaging Interferometer instrument on UARS had a roll and yaw jitter requirement of 4 arc-s/2 s (i.e., 4 arc-s during a 2-s window), which was the minimum spacecraft jitter requirement. All jitter time histories in this paper used a 2-s window duration. Figures 4 and 5 (from the May 1, 1992, experiment) show the roll and yaw jitter response during the ascending part of two orbits in the experiment. During the approximately 34-min period (78,973–81,000 s past start of day, GMT) when all major disturbances known before launch were quiescent, roll jitter exceeded 15.0 arc-s/2 s, and yaw jitter exceeded

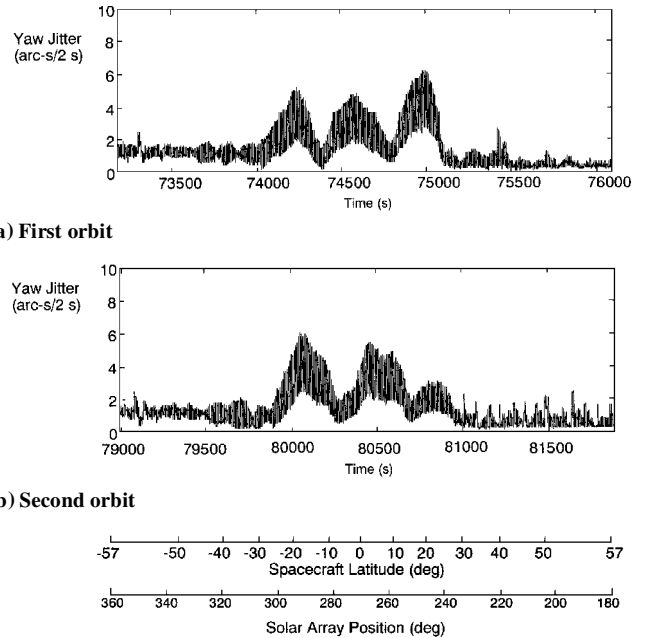


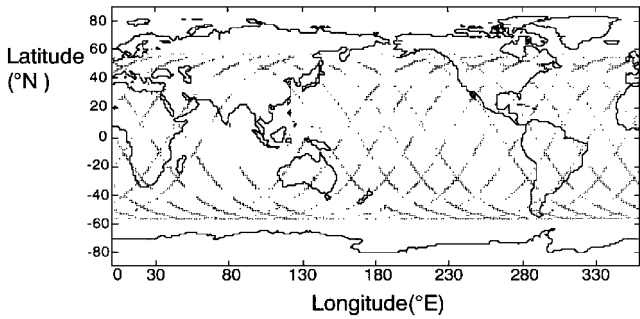
Fig. 5 Yaw jitter at latitudes 57°S to 57°N during ascending part of both orbits in the experiment.

6.0 arc-s/2 s (Figs. 4b and 5b). Figures 4 and 5 also show repeated 5-min (approximately) beats for roll and yaw. Furthermore, power spectral density frequency analysis indicated strong excitation of the solar array fundamental flatwise and edgewise modes.

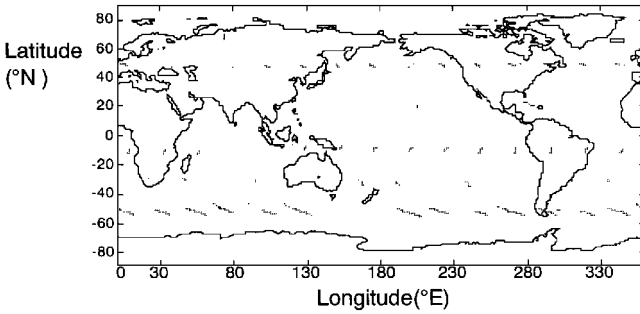
The figures also show the response with respect to spacecraft latitude and solar array position. Because the solar array rotated once per orbit, any anomalies it experienced that were specific to a particular solar array position would also be specific to a particular latitude in orbit. Many of the jitter peaks occurred during approximately the same latitudes in orbit. The response for two orbits is shown to demonstrate that the jitter anomalies occur every orbit. The roll jitter response (Fig. 4) had two distinct beats at approximately 20°S and 20°N. In both orbits, the jitter exceeded 15 arc-s. The smaller 5-min beats that came before and after the two major beats were also repeated. The yaw jitter response (Fig. 5) had three distinctive beats at approximately 20°S, 2°S, and 20°N. During most of the yaw jitter beats, the 4 arc-s/2 s jitter requirement was exceeded. None of the anomalies were due to thermal snap of the solar array, which occurred during the descending part of the orbit.

Figure 6 shows mapping of points on the ground track of UARS that exceeded certain jitter level thresholds. These mappings used 15 h of flight data from the 133rd day past launch (Jan. 22, 1992). Data from this day were not part of the experiment. On Jan. 22, 1992, the solar array was rotating in the forward direction. During the May 1, 1992, experiment, the solar array was rotating in the reverse direction. Thresholds are 4 arc-s/2 s (minimum jitter requirement) (Fig. 6a) and 10 arc-s/2 s (Fig. 6b). From Fig. 6, it can be seen that the jitter exceeded the thresholds only at certain latitudes. The 10 arc-s/2 s roll jitter threshold (Fig. 6b) was exceeded at latitudes of 57°S (sunrise thermal snap), 46°N (sunset thermal snap), 10°S, and 38°S.

Analysis of Figs. 4–6 showed that the jitter response was latitude specific with different response characteristics for forward and backward rotation of the solar array. Reference 7 has shown that average jitter for backward solar array rotation was constantly higher than that for forward rotation. The dominant trends in the jitter patterns were independent of any subsystem or instrument dynamics but varied with solar array position. The correlation of jitter to solar array position was constant.<sup>7</sup> However, the correlation of jitter to ground track latitude was valid for short term (approximately 1 day) analysis due to the precession of the orbit. The link between the spacecraft jitter and spacecraft latitude is warranted because many of the science measurements were referenced to latitude. If the measured jitter levels exceeded instrument pointing requirements consistently for certain latitudes, then the impact of the excessive jitter could result in science measurement anomalies

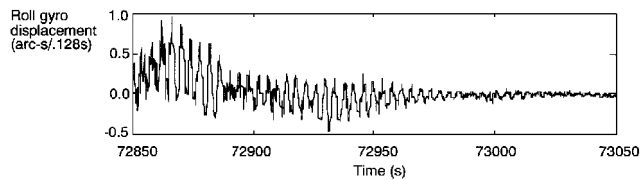


a) Roll jitter exceeding 4 arc-s over a 2-s interval

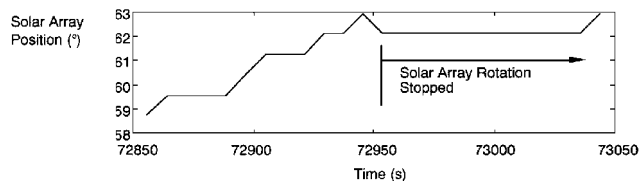


b) Roll jitter exceeding 10 arc-s over a 2-s interval

Fig. 6 Ground track of roll jitter on Jan. 22, 1992.



a) UARS roll response

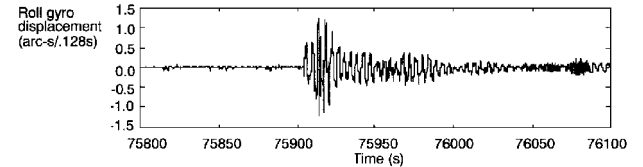


b) Solar array position

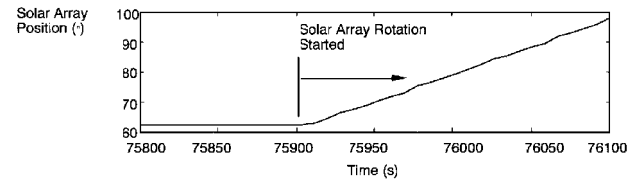
Fig. 7 UARS roll response as the solar array rotation stopped.

being incorrectly attributed to atmospheric phenomena. The latitude of the false measurement anomalies also precessed with orbit. Reference 14 has presented case studies that demonstrated the impact of excessive jitter on science measurements. The aforementioned findings refocused the efforts of the investigation to identify and analyze the excitation source.

On June 2, 1992 (day 265 past launch), after the spacecraft yaw maneuver immediately following the May 1, 1992, experiment, the solar array stopped rotating unexpectedly. It also started rotating approximately 50 min afterward without any commands being given. Figures 7 and 8 (from June 2, 1992, flight data) show the solar array position and the spacecraft roll displacement as the solar array stopped and as it started again, respectively. Before stopping at approximately 72,950 s, the roll gyro measured attitude displacements that exceeded 1.0 arc-s during the 0.128-s sampling intervals. The significant reduction in jitter when the solar array stopped rotating validated the conclusion that the solar array drive was the source of jitter. When the solar array started rotating again, the impulse resulted in roll attitude displacements in excess of 1.2 arc-s during the 0.128-s sampling intervals. Furthermore, the roll displacement exceeded levels of 0.5 arc-s, 50 s after the impulse. The prime contractor for the UARS, General Electric, investigated the cause of the anomaly. They found that the solar array drive stepper motor output,



a) UARS roll response



b) Solar array position

Fig. 8 UARS roll response as the solar array rotation started.

which had 23 pulses/s, transmitted through the harmonic drive, which had a 100:1 reduction ratio, produced a harmonic drive output of 0.23 pulses/s. The harmonic drive output frequency resonated the solar array edgewise and flatwise modes. Stopping the solar array eliminated the excitation source. The reduction in vibration also reduced the solar array flexing being transmitted back to the gear drive.

Reference 5 had measured the free-decay damping of the spacecraft response to the solar array stopping to be 2.8% and had attributed this damping to the solar array edgewise mode of vibration. However, the friction in the gear drive was the probable cause of the high-damping ratio. Because the edgewise mode of vibration was constrained by the gear drive, all of these damping effects would have significantly attenuated structural vibration of the solar array edgewise mode. Furthermore, when the gear drive clutch was locked and other disturbances were active, there was no high value of damping observed for the solar array flatwise and edgewise modes. The damping effect of the gear drive countered the resonating effect of the solar array harmonic drive output. Friction in the gear drive attenuated energy placed into the solar array at the resonant frequency by the harmonic drive. The result was that the solar array had large but bounded levels of vibration. Therefore, any catastrophic damage to the solar array drive was prevented. However, the excessive flexing of the solar array transmitted through the gear drive could reduce the life of the solar array drive.

### Solar Array Modal Contribution to Spacecraft Dynamic Response

The two fundamental solar array modes of vibration dominated the spacecraft motion response. An objective of this investigation was to determine which mode had a larger contribution to the response. Because the only sensors suitable for this study (in terms of frequency and resolution) were the spacecraft gyros, vibration modes could not be identified from measurements alone. To determine which solar array mode dominated the response, the following reasoning was used. Although the solar array harmonic drive output frequency (0.23 Hz) was near the resonant frequencies of the solar array flatwise and edgewise modes (0.2–0.3 Hz), the solar array harmonic drive torque output was almost orthogonal to the flatwise mode but not to the edgewise mode. Because the modes are nearly mutually orthogonal, one can examine the response for the roll and yaw axis at the solar array positions that are 90 deg apart.

When the solar array was at the 180- or 360-deg position, the flatwise mode vibrated about the yaw axis and the edgewise mode vibrated about the roll axis (Figs. 4 and 5). At the 270-deg position, the flatwise mode vibrated about the roll axis and the edgewise mode vibrated about the yaw axis. Figure 2 shows the solar array at the 270-deg position. If the flatwise mode dominated the response, one should expect to see a roll amplitude higher at the 270-deg position than at the 180- and 360-deg positions. Similarly, if the edgewise mode dominated the response, one should expect to see a yaw amplitude higher at the 270-deg position than at the 180- and 360-deg positions. At approximately 240 and 300 deg, both modes contributed to the roll and yaw jitter response that resulted in the

higher amplitudes. The roll jitter amplitude was higher at the 180- and 360-deg positions than it was at the 270-deg position. Yaw jitter amplitude was higher at the 270-deg position than it was at the 180- and 360-deg positions. Therefore, one can infer that the edgewise mode was the dominant mode of vibration.

### High-Gain Antenna Drive Contribution to Spacecraft Dynamic Response

Flight data revealed that the high-gain antenna experienced stiction (static friction), as shown in Fig. 9. At approximately 4720 s, the discontinuity in the periodic waveform was caused by the antenna overcoming static friction. Overcoming the stiction produced an impulse and subsequent roll jitter response of 0.8 arc-s. In addition to the stiction, the high-gain antenna harmonic drive was also a disturbance source. Because of the June 2, 1992, solar array anomaly, the solar array was placed in an active control mode, and then its rotation was stopped such that it would maximize solar incident energy while stationary. It remained in this position for 42 days. However, during this time, isolated high-gain antenna disturbances were then observed and analyzed.

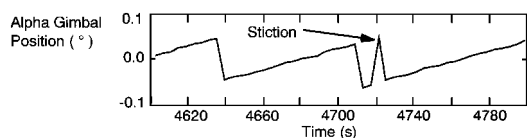
The harmonic drive output frequency  $\omega_{HD}$  (Hz) for a payload having a rotational speed of  $\dot{\theta}$  (deg/s) was

$$\omega_{HD} = \frac{2\dot{\theta}N_{HD}N_{SG}}{360} \quad (1)$$

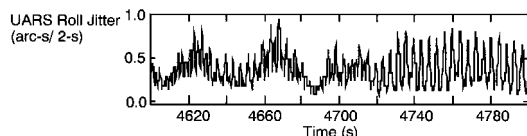
where  $N_{HD}$  and  $N_{SG}$  were the speed reduction ratios for the harmonic drive and the spur gear, respectively. The preceding expression represented the case where the harmonic drive speed reduction preceded that of the spur gear. The solar array reduction ratios,  $N_{HD}$  and  $N_{SG}$ , were 100 and 6.81, respectively. The high-gain antenna and the Solar/Stellar Pointing Platform reduction ratios,  $N_{HD}$  and  $N_{SG}$ , were 200 and 3.24, respectively. The Solar/Stellar Pointing Platform was a gimballed instrument containing three UARS science instruments. The solar array, the high-gain antenna, and Solar/Stellar Pointing Platform targeting/tracking rotational speeds of approximately 0.06 deg/s produced harmonic drive output frequencies of 0.23, 0.22, and 0.22 Hz, respectively. The output frequencies resonated the solar array flatwise and edgewise modes (Fig. 3). The high-gain antenna positioning (rewind) rotational speed of 0.31 deg/s produced a harmonic drive output frequency of 1.12 Hz, which resonated modes 6 and 7 (Fig. 3).

The effect that the high-gain antenna harmonic drive had on jitter is shown in Figs. 9 and 10 using data from the 266th day past launch (June 3, 1992). The high-gain antenna was targeting one of the tracking data and relay satellite spacecraft from 4600 s (past start of day, GMT) to approximately 5350 s. Afterwards, it positioned itself for the other tracking data and relay satellite. From 4600 to 4800 s, the high-gain antenna targeting maneuver was an isolated disturbance. Figure 9 shows the time history of the high-gain antenna alpha gimbal with the rotation removed (4600–4800 s) and roll jitter (4600–4800 s) while the high-gain antenna was targeting a tracking data and relay satellite.

Frequency analysis is shown in Fig. 10 for the high-gain antenna targeting and positioning maneuvers using roll and pitch gyro data.

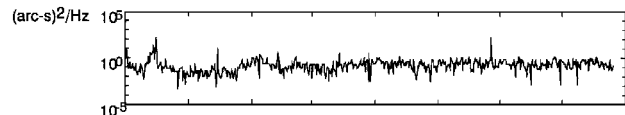


a) High gain antenna alpha gimbal position (with rotation removed) during tracking and data relay satellite targeting

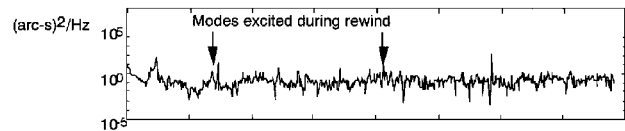


b) UARS roll jitter response during high gain antenna targeting

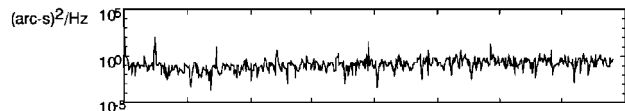
Fig. 9 UARS roll jitter response during high gain antenna targeting and alpha gimbal stiction.



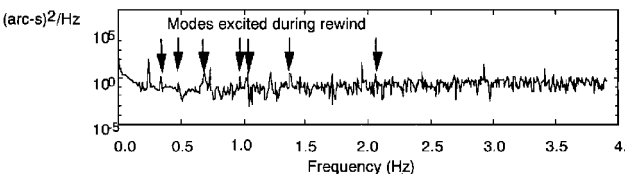
a) UARS roll response during high gain antenna targeting



b) UARS roll response during high gain antenna rewind



c) UARS pitch response during high gain antenna targeting



d) UARS pitch response during high gain antenna rewind

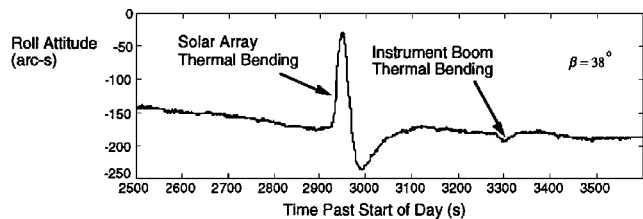
Fig. 10 UARS attitude response during high gain antenna targeting and rewind.

Figures 10a and 10c show the power spectral density of the roll and pitch gyro data, respectively, during the targeting maneuver. The figures indicate that the harmonic drive on the high-gain antenna was also an excitation source of the solar array edgewise and flatwise modes. Figure 9b shows that the jitter was up to 1.0 arc-s/2 s during targeting. From 5600 to 5800 s, the only disturbance present was the high-gain antenna during its positioning (rewind) maneuver. Figures 10b and 10d show the power spectral of the roll and pitch gyro data, respectively, during the positioning maneuver. The modes excited by the positioning maneuver are annotated. During the positioning maneuver, the modes near approximately 0.7, 0.95, and 1.1 Hz were excited. Although 1 arc-s is small with respect to the UARS pointing requirement of 4 arc-s, the identification of the disturbance is important for future spacecraft because the response amplitude will be higher if the disturbance has a higher transmission to the solar array modes or if the spacecraft size is smaller.

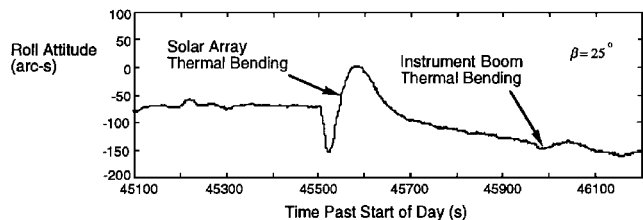
### Appendage Thermal-Elastic Bending Contribution to Spacecraft Dynamic Response

The paper thus far has presented results of analyzing disturbances produced by the spacecraft and the subsequent spacecraft response. This final section presents analysis of the environmental disturbance that resulted from the temperature gradient that was created when a spacecraft entered or exited the Earth's terminator. As a spacecraft's solar array entered sunlight, the side facing the sun heated at a faster rate than the side not facing the sun.<sup>11,12</sup> The thermal gradient caused the appendage to bend away from the sun. As the spacecraft entered the Earth's shadow, the side facing the sun cooled more rapidly than the other side. The thermal gradient caused the array to bend in the opposite direction. The thermal bending produced a torque that changed the attitude of the spacecraft due to conservation of angular momentum. The spacecraft attitude control system responded to the change in attitude with a correcting torque, which restored the spacecraft's nominal attitude.

The analysis of flight data indicated that both elastically flexible appendages experienced thermal elastic bending (thermal snaps) as the spacecraft crossed the Earth's terminator. Figure 11 shows the roll attitude response during two orbital sunrises for two orbits (on days 139 and 370 past launch) with different  $\beta$  angles. The angle  $\beta$  was defined as the complement of the angle between the orbit normal and the Earth-to-sun vector.<sup>12</sup> These angles are indicated



a) Thermal bending on the 139th day after launch



b) Thermal bending on the 370th day after launch

Fig. 11 UARS attitude response to thermal elastic bending of the solar array and instrument boom.

in Figs. 11a and 11b. The solar array thermal snaps were the most pronounced events recorded with the spacecraft's gyros. The solar array bending resulted in a larger attitude displacement about the roll axis. This was caused by the solar energy incident on the large surface area of the array panel and the panel's large mass moment of inertia about the spacecraft roll axis. The solar array temperature gradient and the resulting spacecraft attitude displacement was also inversely dependent on  $\beta$  (Refs. 7 and 12). The initial peaks in Fig. 11, caused by solar array thermal bending, were approximately 125 and 75 arc-s for  $\beta = 38$  and 25 deg, respectively.

In addition to thermal bending, the solar array shadow temporarily shielded the instrument boom containing the Zenith Energetic Particle System from the sun. This resulted in the thermal elastic bending of that boom being delayed by 300–400 s. The delay varied inversely with the angle  $\beta$ . The boom bending effects were less pronounced because of the smaller solar incident surface area and smaller mass inertia. Furthermore, the bending stiffness for the instrument boom was an order of magnitude higher than that of the solar array.<sup>7</sup> Much attention had been focused on the solar array thermal bending and its effect on the science measurements. However, the boom produced a roll attitude displacement of 12 arc-s.

### Concluding Remarks

This paper presented results of investigating in-flight dynamics that occurred within the first 370 days after launch of UARS. The investigation included a three-orbit experiment on May 1, 1992, which measured responses caused by disturbances on the satellite. The solar array and the high-gain antenna harmonic drives were identified as the excitation sources. High-gain antenna stiction was also identified.

The solar array harmonic drive output frequency resonated the solar array edgewise and flatwise structural modes with higher transmissivity to the edgewise mode. The solar array edgewise mode was the dominant mode of vibration. The response was latitude-specific with different jitter characteristics for forward and reverse rotation of the solar array. Because the edgewise mode of vibration was constrained (less slippage and flexing) by the solar array gear drive, the drive damping countered the resonating effect of the solar array harmonic drive output. The solar array had bounded levels of vibration that exceeded the spacecraft pointing requirements. Because of the drive damping, catastrophic damage to the solar array was prevented. However, the flexing of the solar array panel transmitted through the gear drive may have reduced gear drive life.

Analysis of the high-gain antenna showed that its drive excited the solar array edgewise and flatwise modes during targeting and two other structural modes during positioning (rewind). The high-gain antenna also experienced stiction (static friction), which also produced a measurable disturbance. Although the jitter (up to 0.8 arc-s) was far less than that caused by the solar array, the amount was large enough to consider in the overall jitter budget of smaller spacecraft that must maintain pointing requirements similar to UARS.

Analysis of flight data indicated that both elastically flexible appendages experienced thermal elastic bending as the spacecraft crossed the Earth's terminator. Furthermore, the solar array provided a temporary shield between the boom containing the Zenith Energetic Particle System and the sun. This shield resulted in the thermal elastic bending of that boom being delayed by 300–400 s. The displacement was inversely dependent on the beta angle,  $\beta$ .

### Acknowledgments

The authors thank the following people for their assistance and support: William L. Grantham, Jerry Newsom, John G. Wells Jr., Sudha M. Natarajan, and Janet L. Barnes of NASA Langley Research Center; Ansel Butterfield of Bionetics; Richard Quinn, John Molnar, Anthony Camello, Eric Tate, Mike Garnek, Robert Hughes, John Stetson, Lara Phillip, and George Futchko of Lockheed Martin Corporation; Farrell Scott of Florida A&M University; and Richard Beck, Robert Neff, and Sandy Austin of NASA Goddard Space Flight Center.

### References

- Neste, S. L., "UARS Pointing Error Budgets," General Electric Co. Astro-Space Div., PIR U-1K21-UARS-517, Valley Forge, PA, July 1986.
- Anon., "Upper Atmosphere Research Satellite Project Data Book," General Electric Co. Astro-Space Div., Valley Forge, PA, April 1987.
- Anon., "Upper Atmosphere Research Satellite Command and Telemetry Handbook," General Electric Co. Astro-Space Div., SDS-4219, Valley Forge, PA, Jan. 1991.
- Woodard, S. E., Garnek, M., Molnar, J. D., and Grantham, W. L., "The Upper Atmosphere Research Satellite Jitter Study," Flight Experiments Technical Interchange Meeting, Monterey, CA, Oct. 1992.
- Molnar, J., and Garnek, M., "UARS In-Flight Jitter Study for EOS," NASA CR 191419, Jan. 1993.
- Butterfield, A. J., and Woodard, S. E., "Measured Spacecraft Instrument and Structural Interactions," *Journal of Spacecraft and Rockets*, Vol. 33, No. 4, 1996, pp. 556–562.
- Woodard, S. E., "The Upper Atmosphere Research Satellite In-Flight Dynamics," NASA TM 110325, Feb. 1997.
- Harding, R. R., "The Normal Mode Control Law for UARS," General Electric Co. Astro-Space Div., PIR U-1K21-UARS-336, Valley Forge, PA, Feb. 1986.
- Mills, R., and Garnek, M., "UARS Dynamic Disturbance Torque Analysis," General Electric Co. Astro-Space Div., PIR U-1K21 UARS-279, PIR U-1R44-UARS-1351, Valley Forge, PA, Nov. 1985.
- Sheldon, K. M., "Disturbance Torque Summary for UARS," General Electric Co. Astro-Space Div., PIR U-1K21-UARS-232, Valley Forge, PA, Sept. 1985.
- Zimbelman, D. F., "Thermal Elastic Shock and Its Effect on Topex Spacecraft Attitude Control," 14th Annual American Astronautical Society Guidance and Control Conf., Keystone, CO, Feb. 1991.
- Lambertson, M., Underwood, S., Woodruff, C., and Garber, A., "Upper Atmosphere Research Satellite Attitude Disturbances During Shadow Entry and Exit," American Astronautical Society Paper AAS 93-319, Aug. 1993.
- Freesland, D., "Upper Atmosphere Research Satellite Attitude Determination and Control," 15th Annual American Astronautical Society Guidance and Control Conf., Keystone, CO, Feb. 1992.
- Woodard, S. E., Gell, D. A., and Lay, R. R., "Measured Spacecraft Dynamic Effects on Atmospheric Science Instruments," AIAA Paper 97-0419, Jan. 1997.

F. H. Lutze Jr.  
Associate Editor